

EMPLOYING TRACKER VIDEO ANALYSIS SOFTWARE TO INCREASE PRECISION IN COLLECTING DATA IN THE PHYSICS LAB

BOGDAN CHIRIACESCU¹, FABIOLA CHIRIACESCU¹, CRISTINA MIRON^{2,*}, CATALIN BERLIC^{2,*}, VALENTIN BARNA²

¹“Nicolae Iorga” High School, Nehoiu, Romania

²University of Bucharest, Faculty of Physics, 405 Atomistilor Street, Magurele, Romania

*Corresponding authors: cristina.miron@fizica.unibuc.ro, cataliniulian.berlic@g.unibuc.ro

Received

Abstract. Recent advances in affordable video technology have created opportunities to enhance the precision and educational value of physics experiments. This study investigates the use of Tracker Video Analysis software to improve data collection accuracy in the parallel axis theorem laboratory experiment. A rigid circular disc undergoing torsional oscillations was recorded with a high-resolution camera, and frame-by-frame analysis was performed to determine oscillation periods, torsional constants, and moments of inertia. Beyond precision, the methodology enables reproducibility, remote analysis, and conceptual understanding by allowing repeated, high-resolution investigation of physical processes. These findings highlight the value of integrating digital video analysis into physics education to bridge classical experiments with modern data acquisition techniques.

Key words: Tracker video analysis, video-based measurement, parallel axis theorem, physics education.

1. INTRODUCTION

Physics, as the experimental and theoretical study of matter and fields, is often perceived as a challenging subject by high school students and by first-year undergraduates in science and engineering. Despite the relative simplicity of many basic experiments and instruments, students frequently struggle with grasping fundamental concepts and interpreting experimental data [1].

Beyond the act of experimental data with traditional instruments - an activity that has its educational valence - the understanding of the mechanisms might be more important to the apprehension of Physics. Sometimes, traditionally, students are limited to reproducing a certain experimental setup, to obtain some data and analyse it mechanically, without really understanding what is going on. With the help of new technologies, namely video analysis, they can better understand the

phenomenon and have a wider view of the experiment [2, 3].

Using video analysis can be a valuable way to overcome numerous physics learning difficulties linked to observing natural phenomena [4, 5]. By integrating experimental data with digital processing, video analysis bridges abstract physics concepts and real-world phenomena, supporting innovative, critical-thinking-oriented teaching methods. As noted by A. Artiningsih and S. Nurohman, its application in physics instruction substantially enhances students' research skills [6]. In our view, the most precise and accessible tool is the Tracker: Video Analysis and Modelling Tool (hereinafter referred to as Tracker), which integrates video analysis with mathematical and physical modelling. Its global use is well documented in numerous didactic studies. The range of subjects addressed with this software is extensive ranging from kinematic and dynamic characteristics and the laws of motion [7-9], using laboratory instruments, vehicles, and robots [10-13], to optical phenomena such as spectral analysis [14]. Furthermore, Tracker has demonstrated its effectiveness in fostering students' transferable skills.

The use of Tracker software in physics experiments offers numerous advantages. The first is measurement precision, which is limited only by the quality of the recorded footage - specifically, the number of pixels per unit length for spatial measurements and the frame rate for time measurements. Multiple experiments have confirmed this high level of accuracy [15-17], and the range of measurable parameters is extensive. The second advantage is the possibility of repetition. If results are unsatisfactory or influenced by external factors, the experiment can be repeated. Furthermore, measurements can be redone to increase accuracy or to focus solely on the valid portions of the recorded experiment. Third, Tracker enables both quantitative and qualitative observations. Qualitative analysis plays a crucial role in understanding phenomena during didactic laboratory work [18]. The software allows zooming in on images, slowing down motion, and highlighting details that might otherwise be missed. Another advantage lies in its capacity to determine a wide variety of physical quantities and to enable their analysis, comparison, and correlation. Finally, Tracker supports the creation of remote laboratories. High-quality video recordings can be shared with students, who then analyse them using the software. This approach is particularly valuable for groups lacking access to fully equipped laboratory facilities.

In this article we show how Tracker Video Analysis software can be employed to increase the precision of data collection in the 'Parallel Axis Theorem' laboratory experiment, allowing accurate determination of oscillation periods, torsional constants, and moments of inertia.

2. THEORETICAL BACKGROUND

2.1 EXPERIMENTAL SETUP AND MATHEMATICAL FRAMEWORK

The experimental setup consists of a rigid circular disc mounted on a torsional support system and designed to perform small angular oscillations about various parallel axes. The disc is equipped with a series of equidistant perforations along a diameter, allowing it to be suspended at known distances from the central axis passing through its center of mass.

The complete setup includes the following components:

- A rigid torsional suspension or spiral spring, which generates a restoring torque proportional to the angular displacement.
- A dynamometer used to apply a known tangential force at a fixed radial distance, allowing calibration of the torsional constant.
- Adjustable levelling screws, ensuring that the disc is perfectly horizontal to minimize systematic errors due to misalignment.
- An optical light barrier and counter, which measures the period of oscillation. In our implementation of the experiment, instead of using the optical gate and counter as in the standard setup, we employed a video camera mounted vertically above the apparatus, aligned perpendicularly to the plane of the disc, see Fig. 1. This camera allowed for continuous visual recording of the disc's oscillatory motion, capturing precise angular displacements over time. The oscillation periods were later extracted through frame-by-frame video analysis using Tracker software. This method enabled accurate identification of the disc's turning points and corresponding time intervals, offering higher temporal resolution and reducing errors associated with manual timing or limitations inherent to single-beam optical sensors.



Fig. 1 – Experimental setup. The full color version may be accessed at <https://rrp.nipne.ro>.

When displaced from equilibrium and released, the disc undergoes torsional harmonic motion governed by the second-order linear differential equation [19]:

$$I \frac{d^2\varphi}{dt^2} + C\varphi = 0 \quad (1)$$

where:

- I is the moment of inertia of the disc with respect to the axis of rotation,
- C is the torsional spring constant of the suspension system,
- $\varphi(t)$ is the angular displacement from equilibrium.

$$\omega = \sqrt{C/I} \quad (2)$$

and hence the period of oscillation:

$$T = 2\pi\sqrt{I/C} \quad (3)$$

2.2 TORSIONAL CONSTANT DETERMINATION

To evaluate the torsional spring constant C , a known force F is applied tangentially at a radial distance r from the axis, producing a torque:

$$M = F \cdot r \quad (4)$$

The torque required to hold the disc at an angular displacement φ is given by Hooke's law for rotational systems:

$$M = C \cdot \varphi \quad (5)$$

By plotting M against φ , the slope yields the value of the torsional constant C .

2.3 APPLICATION OF THE PARALLEL AXIS THEOREM

The moment of inertia of the disc about an axis located at distance a from the center of mass is determined using Steiner's Theorem (Parallel Axis Theorem) [19]:

$$I = I_{CM} + ma^2 \quad (6)$$

where:

- I_{CM} is the central moment of inertia, *i.e.* moment of inertia about an axis passing through the center of the disk,
- m is the mass of the disc,
- a is the perpendicular distance between the rotation axis and the central axis.

Substituting equation (6) into equation (1) and squaring, we obtain:

$$T^2 = \frac{4\pi^2}{C} (I_{CM} + ma^2) \quad (7)$$

This equation suggests a linear relationship between T^2 and a^2 , which can be empirically verified.

2.4 LINEAR REGRESSION METHOD

Equation (7) is of the form:

$$T^2 = A + B \cdot a^2 \quad (8)$$

where:

$$A = \frac{4\pi^2 I_{CM}}{C} \quad (9)$$

$$B = \frac{4\pi^2 m}{C} \quad (10)$$

Thus, by measuring T for various values of a , one constructs a plot of T^2 versus a^2 . A linear regression yields to the slope B and intercept A , from which

both the central moment of inertia I_{CM} and the torsional constant C can be deduced:

This procedure provides an accurate method to determine rotational inertial properties and offers an experimental test of Steiner's Theorem.

3. EXPERIMENTAL SETUP AND WAY OF WORK

The first step was the calibration of the dynamometer. Observing that the readings from the dynamometer are influenced by diverse external factors, we thought that it would be more precise if we also used Tracker software for reading the values of forces implied. First, we took photos of the deformation of the dynamometer for different forces of deformation, see Fig. 2. Then, knowing those deformation forces (weight of known bodies), we correlated it with the deformation and found the coefficient of the dynamometer's spring. This value we employed later in the calculus of forces implied in the experiment.

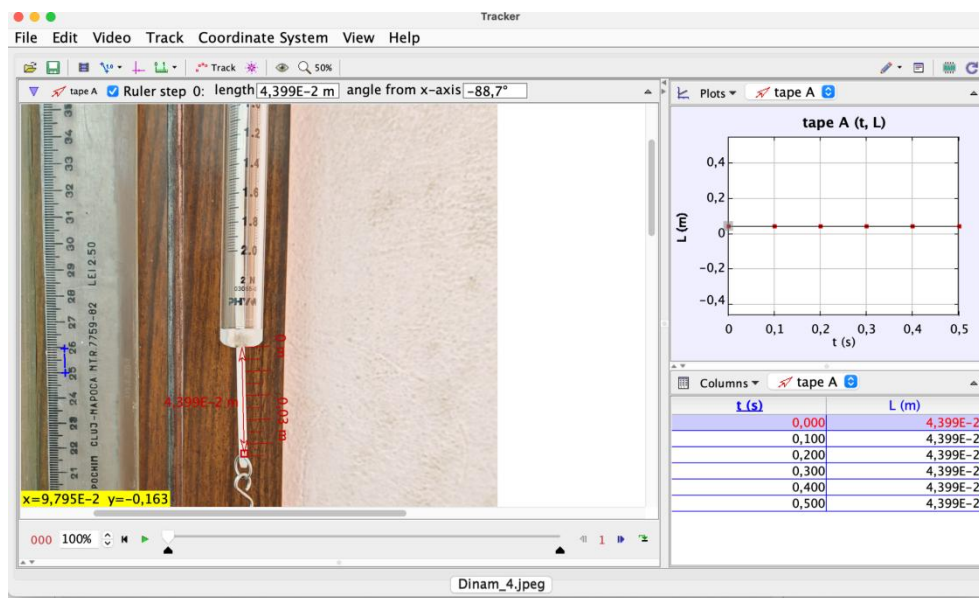


Fig. 2 – Calibration of the dynamometer. The full color version may be accessed at <https://rpp.nipne.ro>.

The next step is finding the elastic coefficient of the spring on which the disk is mounted. For this, we applied for different forces and rotated the disk at different angles, see Figs. 3 and 4.

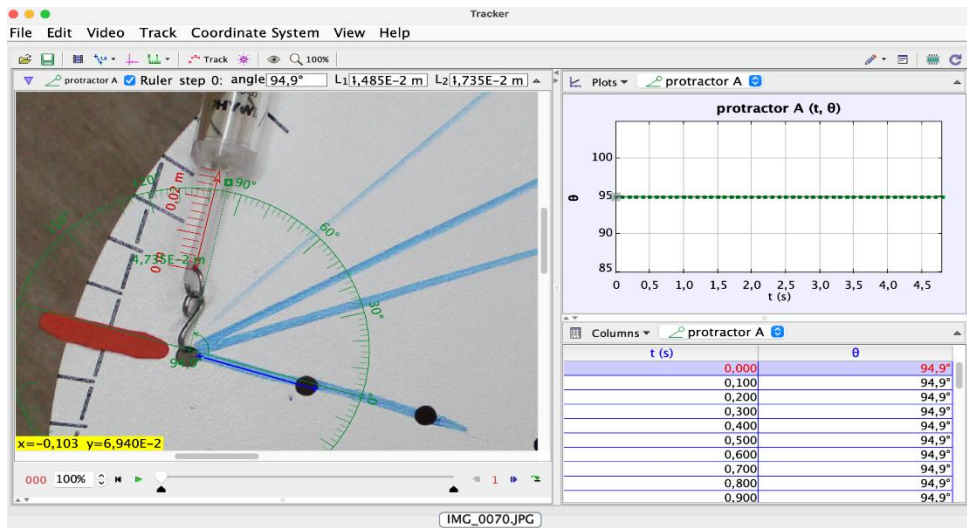


Fig. 3 – Measuring the deformation of the dynamometer to find the force applied. The full color version may be accessed at <https://rrp.nipne.ro>.

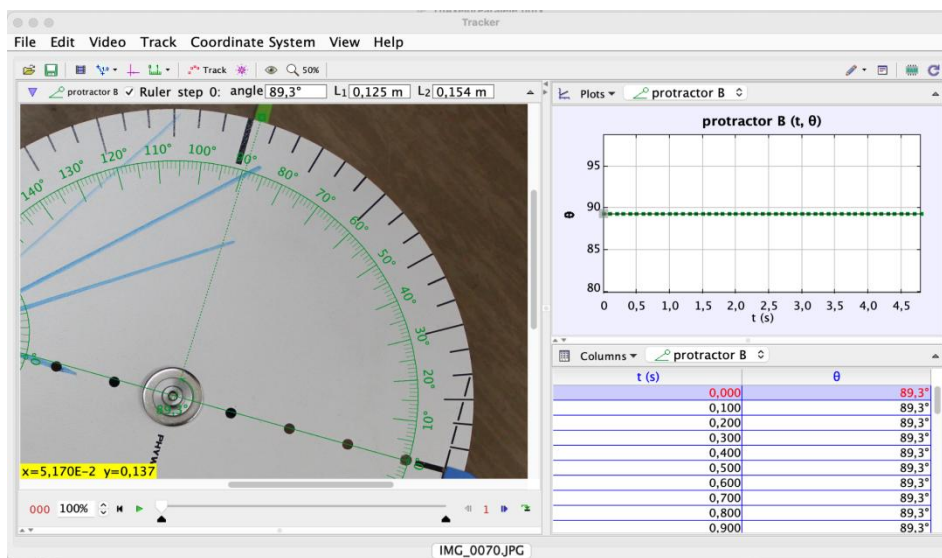


Fig. 4 – Measuring the rotation angle of the disk. The full color version may be accessed at <https://rrp.nipne.ro>.

In Fig 5 is represented the measurement of the angle between the direction of the force and the arm of the force. This is a new feature brought by employing Tracker video analysis. Traditionally, this angle would be appreciated by the experimenter and, of course, the precision would not be great. In this way, we

could introduce all the data in the formula and calculate with greater precision the coefficient.

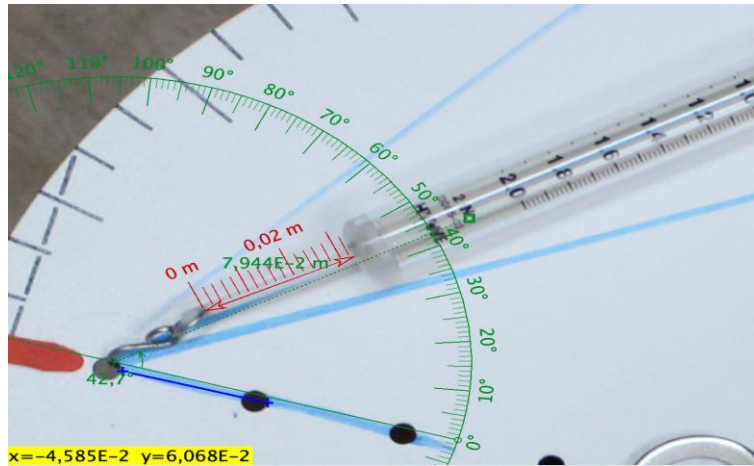


Fig. 5 – Measuring the angle between the direction of the force and force's arm. The full color version may be accessed at <https://rrp.nipne.ro>.

Using this method, we found an average value for $C_{exp} = 0,0256 N \cdot m/rad$. Comparing to the theoretical value, $C = 0,0255 N \cdot m/rad$, we can consider the method a success.

In the second part of the experiment, we can determine the central moment of inertia, I_{CM} , of the metal disk (the moment of inertia with respect to an axis passing perpendicular to the disk, through its center). For this task we have to measure initially the period of oscillation for the disk, when it is fixed in the support in its center of mass, Fig. 6.



Fig. 6 – Experimental setup to measure the oscillation period of the disk. a) general view from above; b) detail with the disk having the oscillation center at the first hole situated at $a = 3\text{cm}$ from the mass center of the disk. The full color version may be accessed at <https://rrp.nipne.ro>.

The oscillating disk was video recorded and then the footage imported into Tracker software. Here, after all the calibrations were made, using the Track command, the evolution of a certain point is followed. In Fig. 7, we can see the outcome of this process.

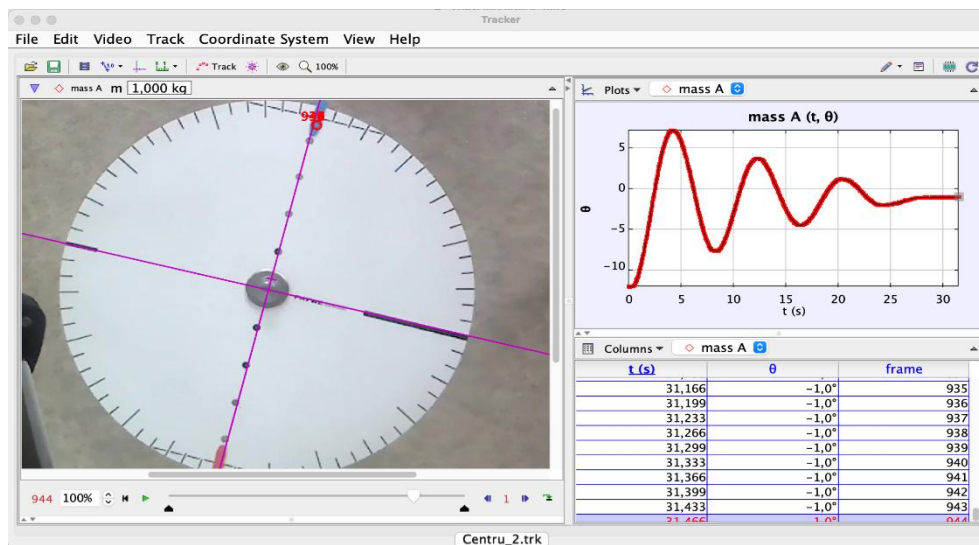


Fig. 7 – Results of tracking process. The full color version may be accessed at <https://rrp.nipne.ro>.

As can be seen on the right part of Tracker window, a graphic is built with the successive positions of the point established to be tracked. Below the graphic, a table containing the moment of time, deviation angle and the frame is made. Both

constructions can be used to find the oscillation period. One way is to identify directly on the graphic points with the same position (e.g. maximum or minimum points of oscillation) and, in this way, to find the period of oscillation. Another approach is to export the data from the table into a spreadsheet program (e.g., Microsoft Excel, LibreOffice Calc) for further analysis.

We employ equation (7), take into account that when the disk is fixed in its center of mass, we have $a = 0$, and we can extract from Tracker the oscillating period T_0 . Knowing already from our previous determinations the value of torsional spring constant C , we can calculate the central moment of inertia, I_{CM} , of our disk.

In Table 1 we present the main results:

Table 1

Central moment of inertia as function of T^2 using equation (7)

No.	T (s)	T^2 (s ²)	I_{CM} (kg · m ²)
1.	2.71700	7.38209	0.00477
2.	2.64080	6.97382	0.00450
3.	2.70025	7.29135	0.00471
4.	2.66700	7.11289	0.00459
5.	2.62421	6.88648	0.00445
6.	2.68367	7.20207	0.00465
7.	2.65582	7.05338	0.00456
8.	2.68010	7.18294	0.00464
9.	2.65040	7.02462	0.00454
10.	2.71030	7.34573	0.00474

We obtain the average value for $\bar{I}_{CM} = 0.00462 \text{ kg} \cdot \text{m}^2$.

Knowing the formula for the theoretical value of $I_{z,th} = 1/2 mR^2$ [19], and measuring the mass of the disk, $m = 0.405 \text{ kg}$, and the disk radius, $R = 15 \text{ cm}$, we can calculate the value of $I_z = 0.00456 \text{ kg} \cdot \text{m}^2$. We acknowledge that the value is similar to the result obtained above in the table via Tracker measurement of the oscillating period.

Furthermore, in this experiment, we can determine the mass of the disk from equation (7) (without using directly a weighing scale), by measuring the oscillation period of the disk with respect to different centers of oscillation, the fasten points being on the disk radius, see Fig 6, but not in the center of mass.

We fitted the disk in the holes situated on its radius at distances $a = 3, 6, 9, 12 \text{ cm}$ from the center of mass. We recorded the oscillating disk and then determined the respective oscillation periods, by employing Tracker software. By employing relation (7) and considering already known from the above table the central moment of inertia, \bar{I}_{CM} one can calculate the value of the disk mass, m .

Table 2 presents the results for the oscillating periods of the disc and the resulting value of the mass. The obtained average result is $m = 0.4183 \text{ kg}$, that is in good agreement with the weighted value of 0.405 kg .

Table 2

Mass of the disk as function of T^2 using equation (7)

No.	$a \text{ (m)}$	$T \text{ (s)}$	$T^2 \text{ (s}^2\text{)}$	$m \text{ (kg)}$
1.	0.03	2.7775	7.71451	0.40886
2.	0.06	3.0738	9.44825	0.41329
3.	0.09	3.5347	12.49410	0.42657
4.	0.12	4.0752	16.60726	0.42444

In Fig. 8, we plot the graph of T^2 v.s. squared distance from the center of mass, a^2 , one can obtain the mass of the disc from the straight-line slope. The slope is equal to $\frac{4\pi^2}{C}m = 660.548 \text{ s}^2/\text{m}^2$, so we can calculate $m = 0.42665 \text{ kg}$. From the plot intercept, one can get the central moment of inertia, I_{CM} . Since the intercept is equal to $\frac{4\pi^2}{C}I_{CM} = 7.107 \text{ s}^2$, thus we find $I_{CM} = 0.00459 \text{ kg} \cdot \text{m}^2$ which is an excellent result.

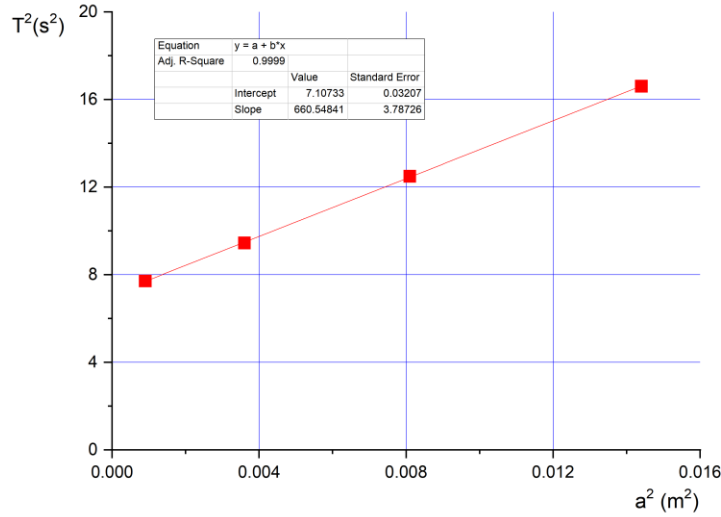


Fig. 8 – Squared oscillating period T^2 as function of squared distance from the center of mass. Full color version may be accessed at <https://rrp.nipne.ro>.

4. CONCLUSIONS

The results of the study demonstrate that the integration of Tracker Video Analysis software into laboratory work significantly improves both the accuracy and interpretative depth of experimental physics measurements. Traditional methods of recording oscillation periods and torsional constants rely on manual timing devices or optical gates with limited resolution, whereas the frame-by-frame approach adopted here minimizes systematic timing errors and allows reproducibility and post-experimental verification of data.

Numerical results support this conclusion. Using the Tracker software to determine the central moment of inertia I_z from oscillation periods measured with the disk fixed at its center of mass, Table 1, we obtained an average value of $I_z = 0.00461 \text{ kg} \cdot \text{m}^2$ which shows excellent agreement with the theoretical prediction $I_{z,th} = 1/2 mR^2$, where the mass $m = 0.405 \text{ kg}$ and radius R were directly measured. The small deviations observed between individual measurements (e.g., from $0.00445 \text{ kg} \cdot \text{m}^2$ to $0.00477 \text{ kg} \cdot \text{m}^2$) are primarily attributed to residual damping and finite frame resolution rather than to systematic bias, highlighting the precision of the method.

Furthermore, by employing equation (7) and plotting the squared oscillation period T^2 against the squared distance a^2 from the center of mass (Fig. 8), we obtained a linear slope of $660.548 \text{ s}^2/\text{m}^2$ from which the mass of the disk was derived as $m = 0.418 \text{ kg}$, a value in very good agreement with the directly measured $m = 0.405 \text{ kg}$, with a relative deviation below 3.2%. Such consistency demonstrates that the combination of Tracker-based oscillation analysis with the Parallel Axis Theorem provides a robust indirect method for determining rotational inertial properties and even fundamental parameters like mass without direct weighing.

Another critical advantage is the ability to measure angles and forces with improved resolution. For instance, using Tracker to determine the angle between the applied force and the lever arm, Fig. 5, removes the subjective estimation errors common in manual angle readings. The dynamometer calibration procedure, enhanced by video analysis as seen in Figs. 2-3, yielded a torsional constant consistent with theoretical expectations, further validating the precision of the approach.

From a didactic perspective, this methodology transforms laboratory work from a purely mechanical exercise into a conceptually driven investigation. Students can now visualize oscillatory motion frame-by-frame, correlate experimental parameters directly with theoretical models, and perform quantitative regression analyses to verify physical laws.

Moreover, the availability of recorded videos enables remote experimentation and repeated analysis, offering substantial pedagogical flexibility

for institutions with limited laboratory access.

These findings confirm that video-assisted experimental analysis bridges the gap between classical physics experiments and modern digital learning tools, ultimately improving both data reliability and student comprehension in physics education.

REFERENCES

1. P. Aguilar-Marín, M. Chavez-Bacilio, S. Jáuregui-Rosas, *Eur. J. Phys.* **39**(3), 035204 (2018).
2. P. Hockicko, L.U. Krišťák, M. Němec, *Eur. J. Eng. Educ.* **40**(2), 145-166 (2015).
3. R. J. Beichner, *Am. J. Phys.* **64**(10), 1272-1277 (1996).
4. G. Tarantino, C. Fazio, *Eur. J. Phys.* **32**(6), 1617-1623 (2011).
5. L. K. Wee, T. K. Leong, *Am. J. Educ. Res.* **3**(2), 197-207 (2015).
6. A. Artiningsih, S. Nurohman, *J. Sc. Edu. Research.* **3**(2), 81-86 (2019).
7. O. S. Sastri, K. S. Swathi, S. Deepa, S. Sharma, *J. Res. (Bede Athenaeum)* **12**(1), (2021).
8. S. Utari, E. C. Prima, *Jurnal Pendidikan Fisika dan Keilmuan* **5**(2), 83-92 (2019).
9. M. Syepudin, R. Badriah, R. Warga, T. Kartini, W. Zikbal, *J. Teach. Learn. Phys.* **3**(2), 14-20 (2018).
10. M. H. Ramli, K. T. Chan, Y. W. Fen, *J. Solid State Sci. Technol.* **24**(2), 297- 305 (2016).
11. P. W. Laws, R. B. Teese, D. P. Jackson, M. C. Willis, K. Koenig, *Scientia in Education* **8**(Special Issue), 223-229 (2017).
12. K. Hockicko, P. Hockicko, J. Ondruš, *Rom. Rep. Phys.* **77**(3), 910 (2025).
13. A Ciobanu, C. Miron, C. Berlic, V. Barna, *Rom. Rep. Phys.* **77**(4), 911 (2025).
14. A. Asrizal, Y. Yohandri, Z. Kamus, *JEP* **2**(1), 41-48 (2018).
15. R. Dumitru, B. Chiriacescu, F. S. Chiriacescu, V. Barna, C. Miron, C. Berlic, *Rom. Rep. Phys.* **76**(4), 906 (2024).
16. P. Aguilar-Marín, G. Rojas-Alegría, C. Morgan-Cruz, M. Chavez-Bacilio, *Rom. Rep. Phys.* **75**(1), 802 (2023).
17. F.S. Chiriacescu, B. Chiriacescu, C. Miron, C. Berlic, V. Barna, *Rom. Rep. Phys.*, **73**(2), 904, (2021).
18. S. Susilawati, M. Satriawan, R. Rizal, S. Sutarno, Fluid experiment design using video tracker and ultrasonic sensor devices to improve understanding of viscosity concept, *International Conference on Mathematics and Science Education 2019 (ICMSCE 2019)*, **1521**, 022039, (2020).
19. R.A. Serway, J.W. Jewett, *Physics for Scientists and Engineers with Modern Physics*, Eight Edition, Cengage Learning, Boston, 2010.